AIAA JOURNAL
Vol. 42, No. 7, July 2004

Size Effects in Metal Foam Cores for Sandwich Structures

Joseph F. Rakow* and Anthony M. Waas†
University of Michigan, Ann Arbor, Michigan 48109-2140

The shear response of aluminum foam, including size effects, is measured and quantified for a closed-cell aluminum foam. The shear stiffness is shown to depend linearly on density, whereas the strength exhibits a power law dependence. The linear response is shown to be independent of strain rate up to rates of 0.17/s, whereas the strength and energy absorption increase with increasing strain rate. The density dependence of the stiffness is reproduced analytically based on the composite cylinders model. Optical techniques are used to measure the strain field of the experimental specimens throughout the loading program. By evaluation of concentric subregions of the sample, a sample size of 18 mean cell diameters is determined to be the dimension below which the uncertainty in the predicted shear modulus of an aluminum foam sample increases significantly. This length scale threshold is replicated in a periodic finite element structure with randomly distributed imperfections.

I. Introduction

METAL foams represent an attractive alternative for sandwich structure cores for multiple reasons. First, with metal foam cores, the adhesive substrate of a sandwich structure may be eliminated with in-production integral bonding to metallic face sheets, stiffening the sandwich and broadening its range of operating environments. Second, metal foams exhibit a compressive stress–strain response that is ideal for energy absorption and impact alleviation with a long, constant stress, plastic strain plateau.[1] Third, an open-cell metal foam offers an opportunity to eliminate the catastrophic nature of water or cryogenic gas permeation that has crippled the long-term use of sandwich constructions with honeycomb cores.[2] Fourth, an open-cell construction also allows for active cooling of the sandwich structure, elevating its range of acceptable operating temperatures.

For integration into sandwich structures, the shear behavior of metal foam must be understood. Some disparate results regarding shear behavior currently exist in the literature. One study found a linear relationship between shear strength and density,[3] whereas a cubic lattice model subjected to shear loading predicted a nonlinear power law dependence.[4] Another investigation offers only a few data points for shear stiffness and strength of melt-foamed aluminum.[5] Furthermore, these experiments involved thin specimens, with no account for size effects.

The present paper offers the full shear response curves for a broad range of density. The density dependence of stiffness and strength are found experimentally with the former being reproduced analytically. The strain rate dependence of the shear response is also considered. The effect of specimen size, relative to the mean cell size, is analyzed experimentally with a unique approach involving digital image correlation. The observed behavior is reproduced with a finite element model. These analyses identify a threshold in the ratio of specimen size to cell size, below which the shear response of a given sample is associated with a significant amount of uncertainty.

Presented as Paper 2003-1946 at the AIAA 44th Structures, Structural Dynamics, and Materials Conference, Norfolk, VA, 7–10 April 2003; received 28 August 2003; revision received 8 January 2004; accepted for publication 9 January 2004.

*Graduate Student Research Assistant, Aerospace Engineering Department. Member AIAA.

†Professor, Aerospace Engineering Department; dcw@umich.edu. Associate Fellow AIAA.

II. Shear Response: Experiments

The details of the experimental procedure and an extended analysis of the results are presented in Ref. 6 by the present authors; a summary is presented here. Square samples of SiC stabilized aluminum foam, produced by Cymat (Ontario, Canada), were subjected to shear loading in the window frame device shown in Fig. 1. Samples ranging in density over 4–15% were tested to obtain the density-dependent relationships for the mechanical properties. Strain rate effects were studied through the low-rate dynamic regime covering the range of $3.65E{-}5$–0.17/s.

A representative response curve, up to and beyond the maximum load, is shown in Fig. 2. The material exhibits a linear region leading to a peak load and a subsequent dramatic loss of load-carrying capability due to large, visible fractures. The postlinear response of aluminum foam in shear is markedly different from its uniaxial response, which exhibits a long constant stress plateau after peak load, leading to densification and a further increase in load-carrying capability.[1] The early onset of plastic deformation, illustrated by the unloading response of Fig. 2 is typical of all metal foam deformation[4] and is generally attributed to the inhomogeneity of the cellular structure of the foam.

The strain rate dependence of the shear response for static loading and for loading with elevated strain rates is shown in Fig. 3 for two samples of like density. The linear response is clearly independent of strain rate within the range of rates investigated, whereas the strength and energy absorption show a slight increase. On average, the samples subjected to elevated strain rates had a specific strength 24% greater and specific energy absorption 36% greater than equivalent samples under static loading.

Figures 4 and 5 show the density dependence and strain rate dependence of the modulus and strength, respectively, of aluminum foam in shear. Eleven samples were tested under static conditions, and five samples were tested under elevated strain rates. The data points in Figs. 4 and 5 represent the complete population of specimens tested in the present study, and the uncertainty of the material parameters is represented by the scatter of these data points. The modulus follows a linear dependence on density and is sufficiently lower than the lower bound of a model presented in Ref. 4. The static strength follows a power law dependence as predicted in Ref. 4. For a complete understanding of the shear strain rate dependence of aluminum foam, the methods employed in the present work must be extended to higher strain rates via, for example, drop tower and split Hopkinson bar experiments.

The sensitivity of aluminum foam to compressive and tensile strain rates have been studied in Refs. 7–11. Static experiments on the uniaxial behavior of aluminum foams were conducted in Refs. 3 and 12–15. References 3 and 5 measured the static shear properties of some aluminum foam samples based on American Society

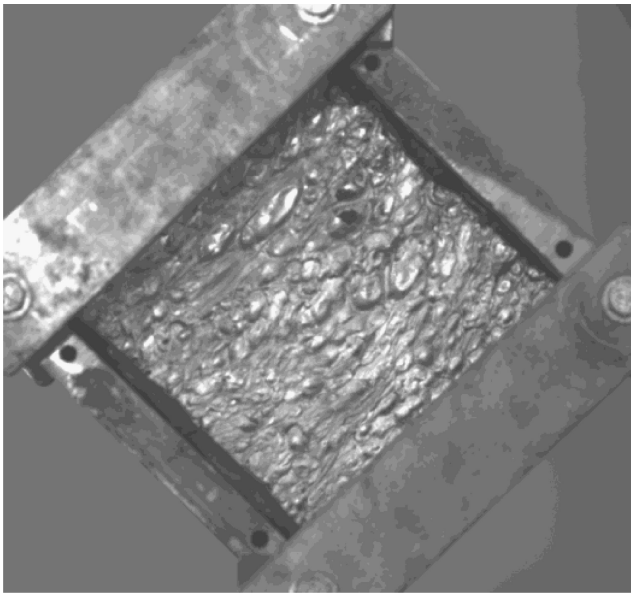

Fig. 1 Loading frame used in shear testing of aluminum foam.

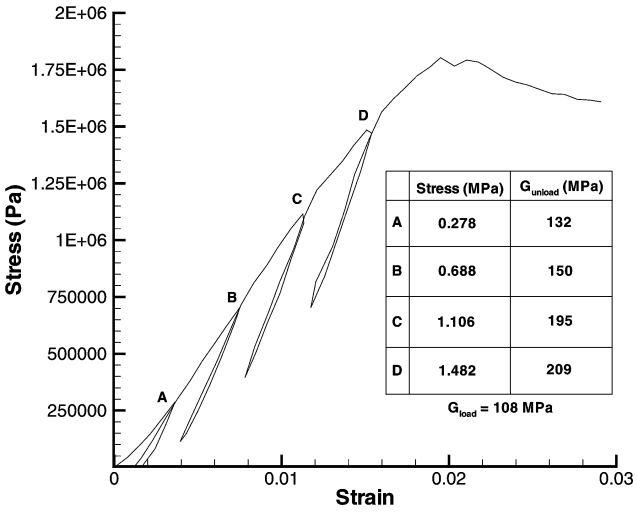

Fig. 2 Representative shear response curve with unloading behavior; plastic strain exists at very low load levels and increases throughout the linear region, stiffening the unloading response.

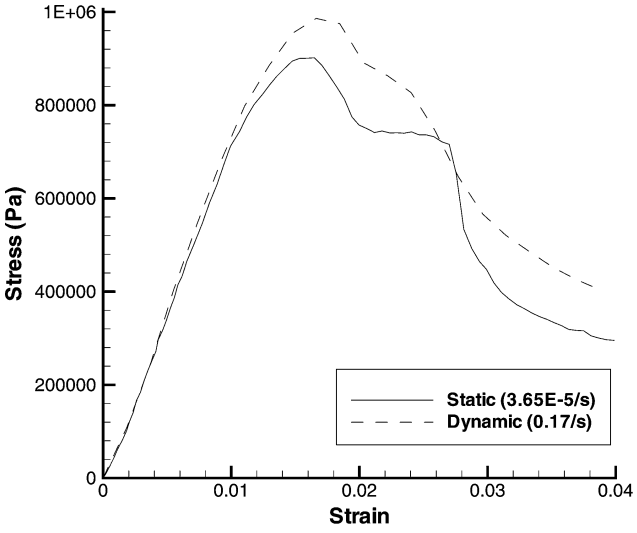

Fig. 3 Comparison between the static and dynamic response curves for two samples of equivalent density.

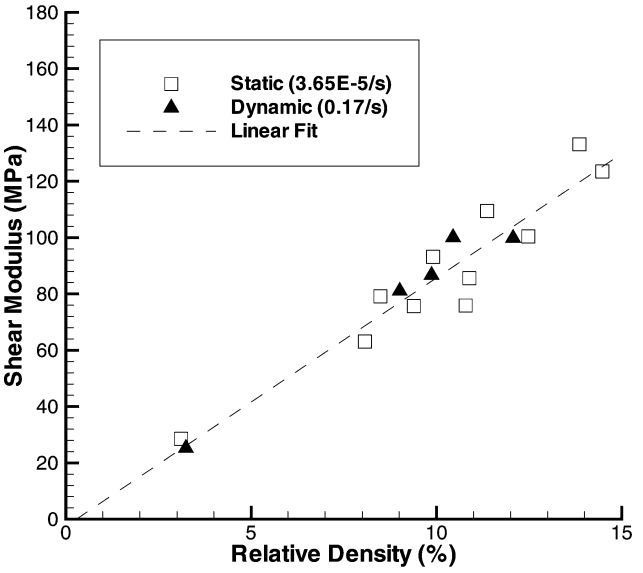

Fig. 4 Shear modulus vs density for static and dynamic loading; no rate effects observed.

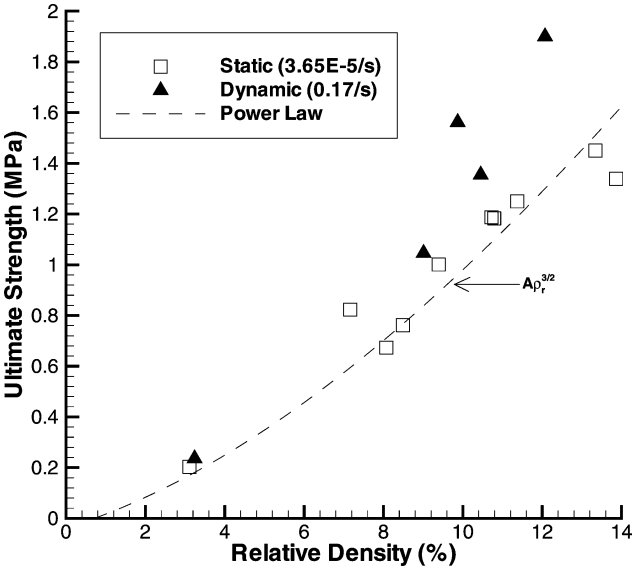

Fig. 5 Shear strength vs density for static and dynamic loading; rate effects observed.

for Testing and Materials C273 without consideration of cell size effects.

III. Shear Response: Analysis

A micromechanical model for the density dependence of the shear modulus of aluminum foam is presented by the present authors in Ref. 16 and is summarized here. The model considers a transversely isotropic representative volume element (RVE) oriented in three-dimensional space. The constitutive properties of the RVE can take various forms such as a concentric cylinder consisting of a fiber surrounded by matrix material or a platelet reinforcement set in a matrix, as shown in Fig. 6. The concentric cylinder may be used to model an open-cell foam or the network of cell edges (where cell edges are the intersection of cell walls) of a closed-cell foam, which have been shown to dominate metal foam deformation.[17] The constitutive properties are evaluated to include cell wall imperfections such as curvature and corrugation, which couples bending and stretching deformation in the cell edges, also consistent with observations.[17] The magnitude of these imperfections and the geometry of the RVE are taken from measurements presented in Ref. 18.

The RVE is subjected to both a state of constant shear strain, following the method of Ref. 19, as well as a state of constant shear

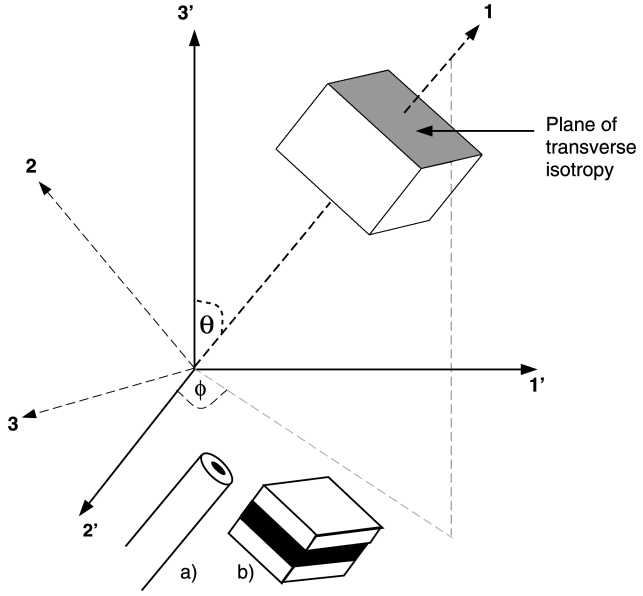

Fig. 6 Transversely isotropic RVE oriented in three-dimensional space: RVE may be a) concentric cylinder or b) platelet-matrix layering.

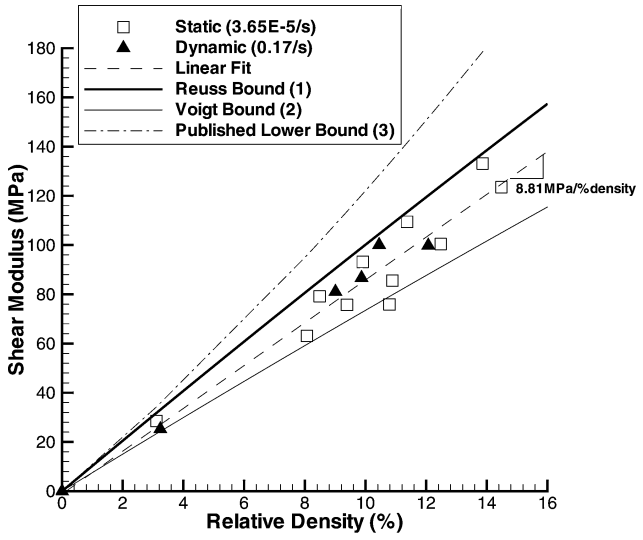

Fig. 7 Model produces appropriate bounds for the experimental shear moduli.

stress. In composite materials, a state of constant strain is an appropriate assumption when the reinforcements are oriented parallel to the direction of loading, whereas a state of constant stress is appropriate when the reinforcements are oriented perpendicular to the direction of loading. For a foam, then, with its load bearing members oriented randomly in space, an analysis of each of these two extremes is appropriate. The assumption of constant stress results in the Reuss bound for the shear moduli and the assumption of constant strain results in the Voigt bound.

The Voigt bound is

$$G_{\text{foam}} = \frac{\rho_r E_s I\left(65 + 4\rho_r \nu_f - 4\rho_r^2 \nu_f^2\right)}{90(1+\rho_f \nu_f)\left(2I + A\sum_n a_n^2\right)} \tag{1}$$

and the Reuss bound is

$$G_{\text{foam}} = \frac{60\rho_r E_s I}{\left(61 + 56\rho_r \nu_f + 4\rho_r^2 \nu f^2\right)\left(2I + A\sum_n a_n^2\right)} \tag{2}$$

in which ρ_r is the relative density of the foam, E_s is the uniaxial modulus of the foam's parent material, I and A are the cross-sectional properties of the cell edges, ν_f is the Poisson ratio of the foam, and a_n are the magnitudes of the sinusoidal imperfections in the foam cell edges, magnitudes that were reported in Ref. 18. A proper extension of the theory leading to Eqs. (1) and (2) is to extend the model to include mechanism-based failure such that the entire shear response may be analyzed.

Within the validity of its assumptions, the model produces an envelope of theoretically acceptable values for the shear modulus of the aluminum foam studied in the present work. The envelope and the experimental data presented are plotted together in Fig. 7. The model and the experimental data agree well. Also plotted is the lower bound of a theory presented in Ref. 4, in which a single cell of a cubic lattice of beam elements is subjected to shear forces, and the equilibrium of forces leads to the relation

$$G_{\text{foam}} = \tfrac{3}{8}(1.0 - 0.1)E_s\left[0.5\rho_r^2 + 0.3\rho_r\right] \tag{3}$$

The lower bound of Eq. (3) is an overprediction of the experimental data.

IV. Size Effects: Experiments

The results presented here and in the related papers are bulk property measurements. In each investigation, the aluminum foam has been treated as a continuous, homogeneous medium, despite obvious inhomogeneities. Regardless of this, such a treatment is valuable if aluminum foam is to be integrated into engineered structures, in which prevailing analysis rests on these very assumptions. When the foam is treated in this manner, congruent to our analysis of materials such as metals, woods, and polymers, it is possible to directly compare the performance of aluminum foam with other competitive engineering materials.

As metals are inhomogeneous on the microscopic level, comprising individual crystals, metal foams are inhomogeneous on the cellular level. When a sufficient amount of the inhomogeneous substructure is considered, that is, a sufficient number of cells, the material acts as a homogeneous continuum. In the present work, experimental measurements related to the shear response are used to determine the length scale at which aluminum foam may be treated as a homogeneous continuum.

The square specimens that were tested in shear, as described earlier, were painted flat white and sprinkled with black glitter to form a random black and white pattern. As the specimen was deformed experimentally, high-resolution black and white digital images (2028×2044 pixels) were captured incrementally. With surface displacement analysis software from the Instron Corporation, the images were segmented into subimages of 32×32 pixels. The software invokes digital image correlation based on the fast Fourier transform to follow the movement of the black and white pattern in each subimage, outputting an average displacement vector for each subimage. This provides a discretized displacement field for the entire surface of the sample.

Shear strains may be evaluated by consideration of square subregions of the sample, concentric with the sample itself, as is shown in Fig. 8. The values for displacement of each point along the edge of the subregion provide the deformation of the edge of the subregion. By interpretation of the change in angle between the edges of the subregion from picture to picture, shear strains may be quantified incrementally, consistent with the definition of engineering shear strain.[20] Through the summation of incremental shear strains, the state of strain in the sample is known at distinct points throughout the loading program.

Subregions of varying size, all concentric with the sample itself, are evaluated for shear strain. The size of the subregion is expressed in mean cell diameters. Measurements of the mean cell diameters for a range of aluminum foam densities are available in Ref. 18 and are used here to define the mean cell diameter. The smallest subregion shown in Fig. 8, for example, has nine mean cell diameters along each of its edges. The next larger subregion is 12 mean cell diameters in size, and so on, by threes.

With the strain known, response curves may be plotted for each subregion, as is shown in Fig. 9, to show the deviation of the local strain state from the global strain state. The results clearly indicate

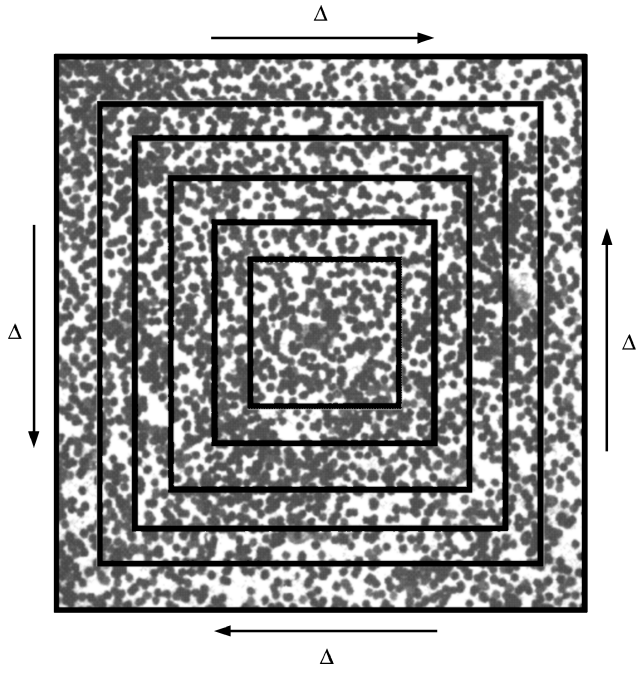

Fig. 8 Black and white patterned specimen with its concentric subregions over which shear strain is calculated. The black lines represent the boundaries of the subregions.

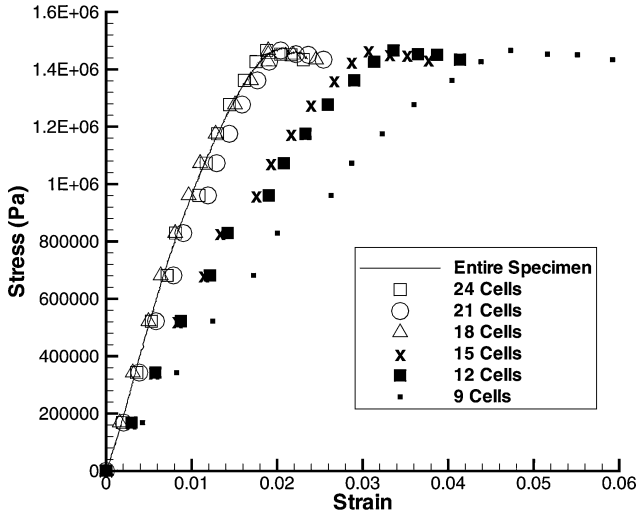

Fig. 9 Shear response of various subregions within a given sample.

that for subregions with dimensions shorter than 18 mean cell diameters, the local stress–strain response deviates significantly from the bulk material response. In contrast, for subregions with dimensions larger than 18 mean cell diameters, the response remains consistent with the bulk properties.

Figure 9 indicates a decline in material stiffness with decreasing sample size, but this is not a general result. Some specimens may even exhibit an increase in stiffness with decreasing sample size. As the sample size decreases, the mechanical behavior of individual cells is magnified because it is no longer averaged out by as many competing neighboring cells. The general result is that the uncertainty in the material response increases as the sample size decreases. This is the essence of mechanical behavior in material samples that are of a size comparable to or smaller than the characteristic dimension.

The experimental result is described further in Fig. 10, in which the ratio ϵ/G_{bulk} is plotted as a percentage vs the number of cells in the subregion. In the ratio, ϵ represents the uncertainty in the shear modulus for a given subregion. The uncertainty is defined as the difference between the shear modulus of the subregion and

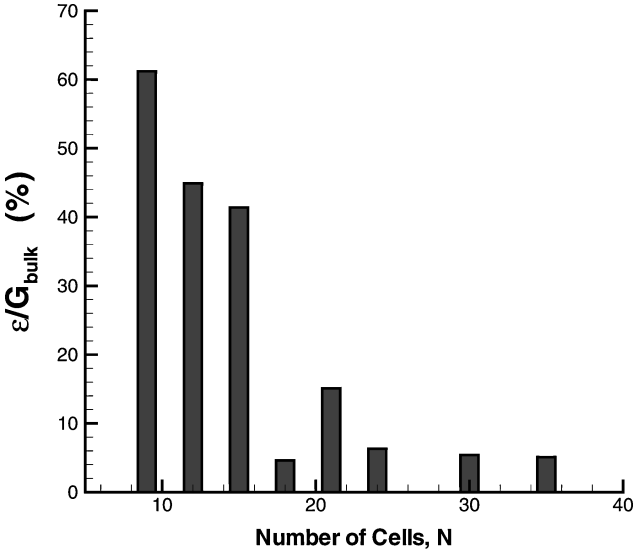

Fig. 10 Shear modulus of the subregions converges to that of the bulk sample as the size of the subregion approaches 18 mean cell diameters.

the shear modulus of the bulk material G_{bulk}. As the number of cells increases, the ratio reaches a value of less than 5% at a subregion size of 18 cells and remains small for all subregions of larger dimensions.

The result presented here compares favorably with results for other macroscopically inhomogeneous materials. In each of Refs. 21–23, it was found that size effects in reticulated foams dominated the sample response if the critical dimension of the sample measured fewer than 20 mean cell diameters.[1]

Optical strain measurement is an ideal method for obtaining size effects for two reasons. First, a broad range of sample sizes may be tested simultaneously and, therefore, subjected to identical test conditions. Second, the ratio of surface area to volume remains constant even though measurements are obtained for samples of varying size. When the samples are machined for the present study and for other studies, cells on the sample edge are damaged. The mechanical integrity of these cells is diminished, yet they still contribute to the overall volume of the sample. The ratio of the damaged edge cells to undamaged cells increases as the machined sample size decreases. In the present method, this ratio remains constant while allowing for the testing of a range of sample sizes.

V. Size Effects: Analysis

The subject of homogenization of inhomogeneous materials is a complex topic that requires a rigorous mathematical approach to obtain a true understanding of its related nuances. Such approaches are summarized in Refs. 24 and 25. The present approach is an attempt to illustrate and replicate, with a simple and sensible model, the size effect behavior observed in the experiments.

In earlier studies, aluminum foam has been modeled as a random structure and as a periodic structure; its cells have been considered perfect as well as imperfect. In Ref. 16, as summarized, the foam is modeled as a random structure with imperfections. In Refs. 1 and 26, among others, it is modeled as a perfect periodic structure. Even though simple observation reveals that aluminum foam is an imperfect, semirandom structure, the results of the preceding section illustrate that the random and imperfect nature of the foam structure is important in shear only for samples with dimensions fewer than 18 mean cell diameters. For a sample smaller than the threshold value, the shear response depends highly on the specific imperfections contained within the subregion. Some imperfections act as stiffening mechanisms, whereas others promote compliance. As the sample size decreases, imperfections dominate, and the uncertainty in the material response increases.

In this section of the present work, a periodic structure of $N \times N$ cells with randomly distributed imperfections is created and analyzed with finite elements. The structure is not meant to model

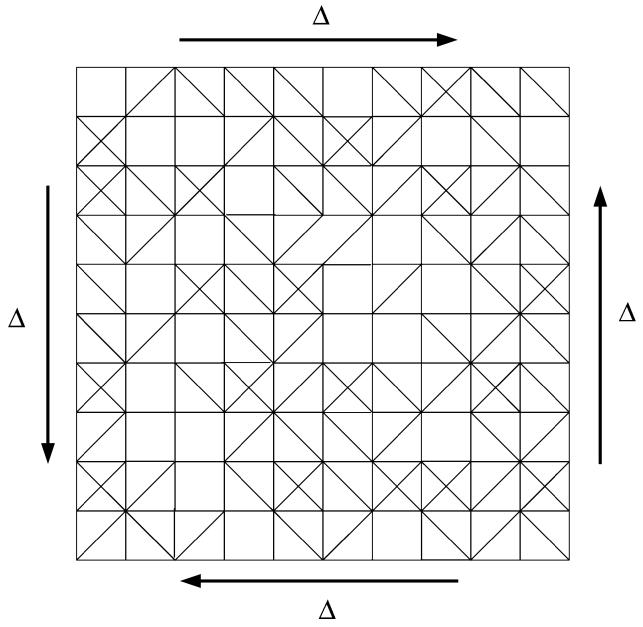

Fig. 11 Finite element model of a 10 × 10 imperfect periodic structure. Geometry of each cell is chosen randomly from the four cells in Fig. 12.

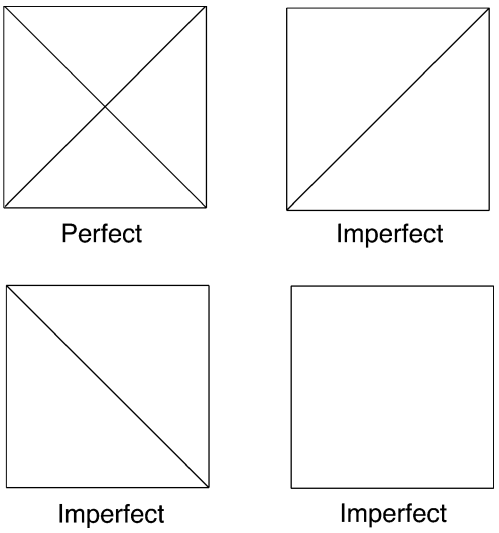

Fig. 12 Four cells that are used to construct a periodic structure with randomly distributed imperfections.

aluminum foam. It is used as a tool to understand the behavior of periodic structures in shear as imperfections are introduced. The uncertainty in shear stiffness of the imperfect structures is of primary concern. The model will be used to observe the disappearance of this uncertainty as the sample size grows (as the number of cells N, increases).

A 10×10 imperfect periodic structure, as an example, is shown in Fig. 11. The structure is made of four basic unit cells, one perfect and three imperfect (Fig. 12), randomly distributed, each with an equal probability of inhabiting any given cellular location. There are 100 (N^2) cell locations. The structure is sheared through a prescribed displacement along the boundary, and the shear stiffness is computed. The structure is then given a different random distribution of cellular imperfections by the use of the same four basic cells, and the shear stiffness is measured again. This is repeated at least three times for each value of N chosen from the range $3 \leq N \leq 50$. For a given value of N, multiple runs, each with its associated distribution of cellular imperfections, produce a range of shear stiffnesses. The magnitude of the range is taken to be the uncertainty ϵ in the

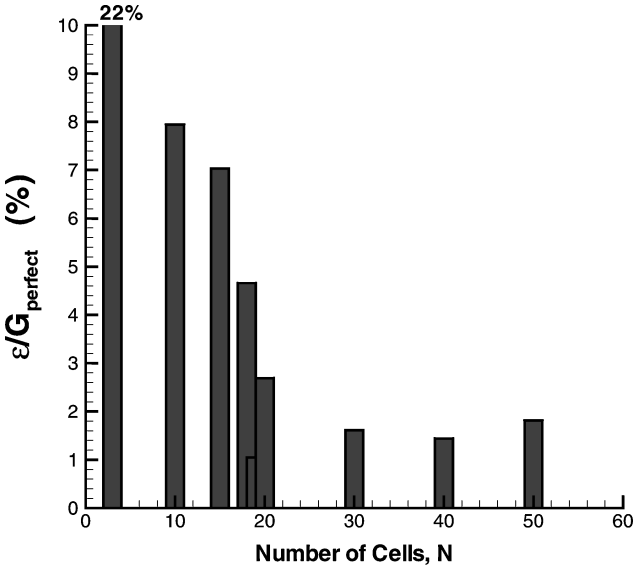

Fig. 13 Uncertainty in the shear stiffness of the imperfect structure in Fig. 11 approaches a constant value for a structure larger than 18 × 18 cells.

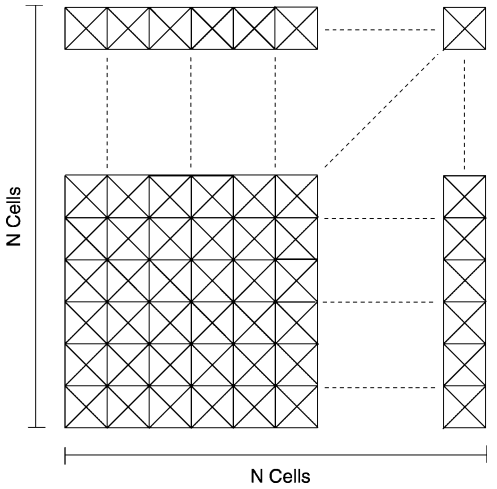

Fig. 14 Perfect periodic structure has $N \times N$ perfect cells.

shear stiffness of the $N \times N$ periodic structure. It was found that no more than three runs for each value of N was necessary to produce a representative range of shear stiffness values.

The models were created and solved in ABAQUS with B23 cubic beam elements with solid rectangular cross sections. The dimensions of the structure were scaled such that the perfect structure had a constant shear stiffness regardless of the value of N.

The ratio $\epsilon/G_{\text{perfect}}$ is plotted vs the number of cells N in Fig. 13, in which G_{perfect} is the shear stiffness of the perfect periodic structure shown in Fig. 14. The histogram in Fig. 13 is remarkably similar to that in Fig. 10. For structures with more than 18 cells in each dimension, the uncertainty in shear stiffness becomes small and remains relatively constant for all larger specimen sizes.

A pertinent response to this result is to consider the degree of imperfection introduced in the preceding model. Perhaps this set of allowable imperfections is such that the uncertainty in shear stiffness just so happens to drop off for sample dimensions larger than 18 cells. Perhaps a more detrimental set of imperfections, that is, imperfections that reduce the shear stiffness of a given sample more drastically than those chosen here, would require even larger sample sizes before the uncertainty in shear stiffness approaches a constant value.

To investigate such a possibility, each beam member of the perfect structure shown in Fig. 14 is given a 50% probability of disappearing

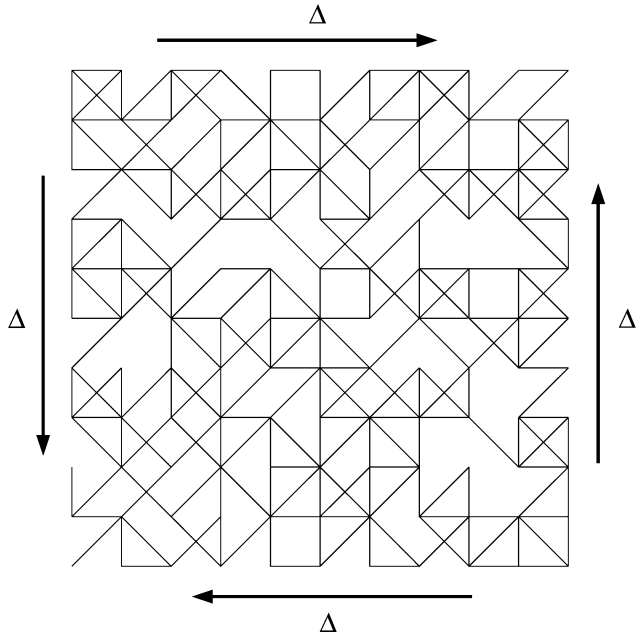

Fig. 15 Finite element model of an imperfect periodic structure in which the imperfections are such that any member of any cell has a 50% probability of being nonexistent.

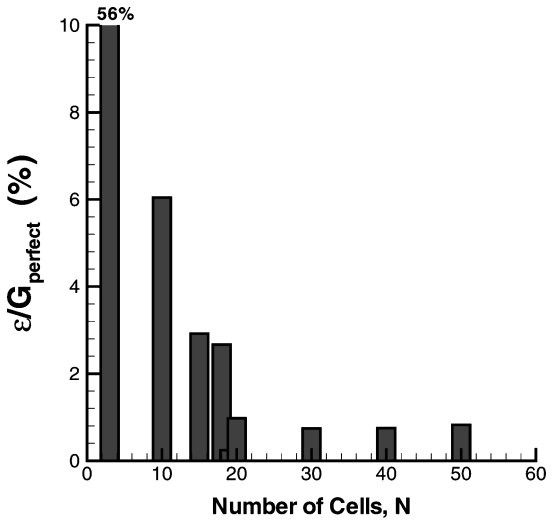

Fig. 16 Uncertainty in the shear stiffness of the imperfect structure in Fig. 15 approaches a constant value for a structure larger than 18 × 18 cells.

from the structure entirely. In the preceding problem, only the cross bars (the diagonal elements of each cell) were given a 50% probability of disappearing, whereas the horizontal and vertical cell members always remained. An example of the newly degraded structure is shown in Fig. 15.

The same procedure of the introduction of three sets of imperfections into each $N \times N$ sample is followed, and the results are plotted in Fig. 16. Clearly, despite the drastic increase in imperfection population, the uncertainty in the shear stiffness of the structure still approaches a constant value when the specimen dimensions are greater than 18 cells. Such results bolster the claim that the shear response of aluminum foams is imperfection-dominated and is, therefore, associated with an increased level of uncertainty for sample sizes of fewer than 18 cells in each direction in the plane of shearing.

Structures of different geometry, that is, honeycombs with circular, hexagonal, or triangular cells, and varying degrees of imperfection would be valuable subjects of study to understand the dependence, if any, of the results presented here on such parameters. The only size effect studies regarding aluminum foam known to the authors are found in Refs. 26 and 27. In Ref. 26, the shear modulus of an analytical regular hexagonal honeycomb structure is analyzed by equilibrium and is shown to converge to have bulk shear stiffness when the number of cells is three or greater through the thickness. Because the model contains perfect cells, the convergence properties do not represent the averaging out of imperfections, as are present in metal foams. Rather, the convergence depends solely on the shape of the cell chosen, in this case, hexagonal honeycomb. In Ref. 27, aluminum foam specimens of varying thickness are sheared experimentally. It is found that the strength of these foams does not depend on specimen thickness for specimens with at least three cells through the thickness.

VI. Conclusions

The results presented in the present paper are intended to reveal the characteristics of aluminum foam that are of primary concern for sandwich structure cores. These are characteristics associated with the shear response of the material and the effect of its cellular strucure on such parameters when sample sizes approach cell sizes. The shear stress–strain response was measured and was shown to have an initial linear region accompanied by an increasing plastic strain even at low load levels. After peak load, the load-carrying capability of the foam dropped off quickly. Up to strain rates of 0.17/s, the linear response was independent of strain rate, whereas the peak load and energy absorption each increased as the strain rate increased. A model based on the composite cylinders model simulated the network of imperfect cell edges and offered an envelope of predicted values for the aluminum foam shear modulus.

Size effects were studied through experiment and simulation. Digital image correlation provided the full displacement field on the surface of the foam throughout the experimental loading program. Shear strain was calculated over concentric subregions of varying size within the sample. For subregions with dimensions shorter than 18 mean cell diameters, the shear response became uncertain. This uncertainty increased as the size of the subregion decreased. The same behavior was observed through a finite element model of a periodic structure with randomly distributed imperfections. For structures with dimensions shorter than 18 cells within the plane of shear, the uncertainty in the shear response increased as the sample size decreased. This behavior was constant for various degrees of cellular imperfection.

References

[1]Gibson, L. J., and Ashby, M. F., *Cellular Solids: Structure and Properties*, Cambridge Univ. Press, Cambridge, England, U.K., 1997, pp. 175–231.

[2]"Final Report of the X-33 Liquid Hydrogen Tank Test Investigation Team," NASA George C. Marshall Space Flight Center, May 2000.

[3]von Hagen, H., and Bleck, W., "Compressive, Tensile, and Shear Testing of Melt-Foamed Aluminum," *Materials Research Society Symposium Proceedings*, Vol. 521, Materials Research Society, Warrendale, PA, 1998, pp. 59–64.

[4]Ashby, M. F., Evans, A. G., Fleck, N. A., Gibson, L. J., Hutchinson, J. W., and Wadley, H. N. G., *Metal Foams: A Design Guide*, Butterworth–Heinemann, Boston, 2000.

[5]Saenz, E., Baranda, P. S., and Bonhomme, J., "Shear Properties of Aluminum Metal Foams Prepared by the Melt Route," *Materials Research Society Symposium Proceedings*, Vol. 521, Materials Research Society, Warrendale, PA, 1998, pp. 83–89.

[6]Rakow, J. F., and Waas, A. M., "Size Effects and the Shear Response of Aluminum Foam," *Mechanics of Materials* (to be published).

[7]Dannemann, K. A., and Lankford, J., Jr., "High Strain Rate Compression of Closed-Cell Aluminum Foams," *Materials Science and Engineering*, Vol. A293, 2000, pp. 157–164.

[8]Hall, I. W., Guden, M., and Yu, C.-J., "Crushing of Aluminum Closed Cell Foams: Density and Strain Rate Effects," *Scripta Materialia*, Vol. 43, 2000, pp. 515–521.

[9]Paul, A., and Ramamurty, U., "Strain Rate Sensitivity of a Closed-Cell Aluminum Foam," *Materials Science and Engineering*, Vol. A281, 2000, pp. 1–7.

[10]Mukai, T., Kanahashi, H., Miyoshi, T., Mabuchi, M., Nieh, T. G., and Higashi, K., "Experimental Study of Energy Absorption in a Close-Celled Aluminum Foam Under Dynamic Loading," *Scripta Materialia*, Vol. 40, No. 8, 1999, pp. 921–927.

[11] Deshpande, V. S., and Fleck, N. A., "High Strain Rate Compressive Behaviour of Aluminum Foams," *International Journal of Impact Engineering*, Vol. 24, 2000, pp. 277–298.
[12] McCullough, K. Y. G., Fleck, N. A., and Ashby, M. F., "Uniaxial Stress–Strain Behaviour of Aluminum Alloy Foams," *Acta Materialia*, Vol. 47, No. 8, 1999, pp. 2323–2330.
[13] Andrews, E., Sanders, W., and Gibson, L. J., "Compressive and Tensile Behaviour of Aluminum Foams," *Materials Science and Engineering*, Vol. A270, 1999, pp. 113–124.
[14] Motz, C., and Pippan, R., "Deformation Behaviour of Closed-Cell Aluminum Foams in Tension," *Acta Materialia*, Vol. 49, 2001, pp. 2463–2470.
[15] Bastawros, A.-F., Bart-Smith, H., and Evans, A. G., "Experimental Analysis of Deformation Mechanisms in a Closed-Cell Aluminum Alloy Foam," *Journal of the Mechanics and Physics of Solids*, Vol. 48, 2000, pp. 301–322.
[16] Rakow, J. F., and Waas, A. M., "The Elastic Moduli of Random Fibrous Composites, Platelet Composites, and Foamed Solids," *Mechanics of Advanced Materials and Structures* (to be published).
[17] Bart-Smith, H., Bastawros, A.-F., Mumm, D. R., Evans, A. G., Sypeck, D. J., and Wadley, H. N. G., "Compressive Deformation and Yielding Mechanisms in Cellular Al Alloys Determined Using X-Ray Tomography and Surface Strain Mapping," *Acta Matrialia*, Vol. 46, No. 10, 1998, pp. 3583–3592.
[18] Simone, A. E., and Gibson, L. J., "Aluminum Foams Produced by Liquid-State Processes," *Acta Materialia*, Vol. 46, No. 9, 1998, pp. 3109–3123.
[19] Christensen, R. M., and Waals, F. M., "Effective Stiffness of Randomly Oriented Fibre Composites," *Journal of Composite Materials*, Vol. 6, 1972, pp. 518–532.
[20] Fung, Y. C., *Foundations of Solid Mechanics*, Prentice–Hall, Englewood Cliffs, NJ, 1965, p. 95.
[21] Lakes, R. S., "Size Effects and Micromechanics of a Porous Solid," *Journal of Materials Science*, Vol. 18, 1983, pp. 2572–2580.
[22] Brezny, R., and Green, D. J., "The Effect of Cell Size on the Mechanical Behavior of Cellular Materials," *Acta Metallurgica et Materialia*, Vol. 38, No. 12, 1990, pp. 2517–2526.
[23] Mora, R., and Waas, A. M., "Strength Scaling of Brittle Graphitic Foam," *Proceedings of the Royal Society of London, Series A: Mathematical and Physical Sciences*, Vol. 458, 2002, pp. 1695–1718.
[24] Manevich, L. I., *Mechanics of Periodically Heterogeneous Structures*, Springer-Verlag, New York, 2002.
[25] Cioranescu, D., *Homogenization of Reticulated Structures*, Springer-Verlag, New York, 1999.
[26] Onck, P. R., Andrews, E. W., and Gibson, L. J., "Size Effects in Ductile Cellular Solids. Part I: Modeling," *International Journal of Mechanical Sciences*, Vol. 43, 2001, pp. 681–699.
[27] Andrews, E. W., Gioux, G., Onck, P., and Gibson, L. J., "Size Effects in Ductile Cellular Solids. Part II: Experimental Results," *International Journal of Mechanical Sciences*, Vol. 43, 2001, pp. 701–713.

A. Palazotto
Associate Editor